

RADIATIVE PION CAPTURE IN NUCLEI*

Helmut W. Baer and Kenneth M. Crowe

Lawrence Berkeley Laboratory
University of California
Berkeley, California 94720

NOTICE

This report was prepared as an account of work sponsored by the United States Government. Neither the United States nor the United States Atomic Energy Commission, nor any of their employees, nor any of their contractors, subcontractors, or their employees, makes any warranty, express or implied, or assumes any legal liability or responsibility for the accuracy, completeness or usefulness of any information, apparatus, product or process disclosed, or represents that its use would not infringe privately owned rights.

ABSTRACT

The process of radiative pion capture has in recent years been shown to be a good probe of nuclear structure. The experiments and theoretical results which support this statement are reviewed. High-resolution data on the photon spectra from nuclei ranging in mass $1 \leq A \leq 209$ are shown. We discuss the observation of giant resonances in $T_z = +1$ nuclei, the quasi-free capture process, and transitions to individual bound nuclear states. The observed transition rates in $1p$ -shell nuclei are compared with recent shell model calculations based on an impulse-approximation Hamiltonian whose amplitudes are not adjustable constants, but are obtained from the fundamental process on the nucleon, $\pi^- + p \rightarrow n + \gamma$. The agreement is good within the limits set by the uncertainties of pionic x-ray data. Some features of radiative π capture on very light nuclei $-A=2, 3$ and 4 -are reviewed. Finally, we discuss the $\pi^- + {}^6\text{Li} (1^+) \rightarrow \gamma + {}^6\text{He} (0^+)$ transition where the PCAC hypothesis and soft-pion limit have been applied. The $1s$ -state radiative capture rate evaluated with these assumptions is found to agree with impulse approximation calculations and is within reasonable agreement with the recent data when corrections for $2p$ capture are made.

INTRODUCTION

The question to which we draw your attention is: what can be learned about nuclear structure by stopping negatively charged pions in a target and examining with 2-MeV resolution the emitted photon spectrum in the region of 50 to 140 MeV? Processes which produce photons in this region are radiative capture:

$$\pi^- + A_i \rightarrow A_f + \gamma \quad (1a)$$

$$\rightarrow (A-1)_f + n + \gamma \quad (1b)$$

$$\rightarrow (A-2)_f + n + n + \gamma \quad (1c)$$

⋮

and charge exchange

$$\pi^- + A_i \rightarrow A_f + \pi^0 \quad (2)$$

The latter has only been observed with hydrogen and ${}^3\text{He}$. Study of hydrogen and deuterium in the early 1950's helped determine basic properties of the pion, such as its mass, odd intrinsic parity, and πN coupling strength. In recent years targets ranging up to $A = 209$ have been

studied and some of the interest has turned to the study of nuclear structure.

The study in 1966 by Davies *et al.*¹ with a large NaI detector demonstrated that the branching ratios for reactions (1) for pions in bound atomic orbits is $\sim 2\%$. A summary of measured values for both reactions (1) and (2) is given in Table I. The basic fact established by observation of the high-energy photons is that the reactions of Eq. (1) occur as a direct interaction (rather than through formation of a compound nuclear state) of a π^- with a proton in the nucleus, the fundamental process being $\pi^- + p \rightarrow n + \gamma$. With this knowledge one could anticipate that the impulse approximation might be valid, and thus one had a reasonably good idea of what transition operator to use in calculating the radiative transition for nuclei. Recognizing the similarity between the dominant term of this operator,

$\tau_+ \vec{\sigma} \cdot e i \vec{k} \cdot \vec{r}$, with the electric dipole operator in photonuclear reactions, several authors² predicted that the well-known giant-dipole resonances should be selectively and strongly excited. Motivated by these predictions, the Berkeley group³ set up a high-resolution electron-positron

*Work performed under the auspices of the U. S. Atomic Energy Commission.

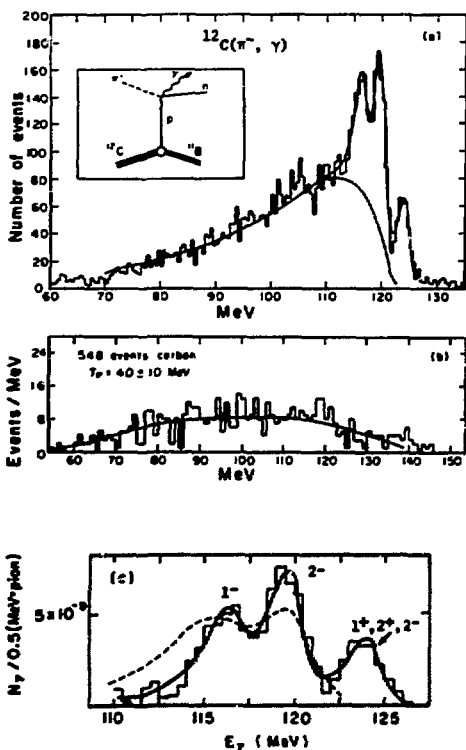
M.A.S. 111

44

Table I. Radiative and charge exchange branching ratios^a for stopped π^- absorption on nuclei.

Target nucleus	Radiative (R_γ) (%)	Charge exchange (R_{n^0}) (%)	Atomic capture ^b orbitals
^1H	39.5 ± 3^c	60.5 ± 3^c	1s
^2H	24.7 ± 7^c	$.08 \pm 1.0^d$	1s
^3He	13.9 ± 1.9	18.6 ± 2.3	1s, 2p
^4He	1.50 ± 0.09	Q forbidden	1s, 2p
^6Li	4.39 ± 5.8	$< .4\%$ ^c	1s, 2p
^7Li	1.9 ± 2^f	$.003^c$	1s, 2p
^{12}C	1.92 ± 2.0	Q forbidden	1s, 2p
^{14}N	2.24 ± 4.8	$< .5\%$	1s, 2p
^{16}O	2.24 ± 4.8	Q forbidden	1s, 2p
^{24}Mg	2.15 ± 4.3	Q forbidden	1s, 2p (3d)
^{32}S	1.8 ± 1^f		2p, 3d
^{40}Ca	1.94 ± 3.5	$< .5\%$	2p, 3d
$^{63,65}\text{Cu}$	1.5 ± 1^f		2p, 3d
^{209}Bi	1.57 ± 5.2	$< .5\%$	4f, 5g

^a Values from Ref. 3 except where otherwise indicated. ^b Backenstoss³⁵ (1970). ^c Ryan¹⁹ (1963). ^d Chinowsky *et al.*³⁶ (1954). ^e Petrukhin *et al.*³⁷ (1964). ^f Davies *et al.*¹ (1965).



tron pair spectrometer at the LBL 184-inch cyclotron, and were able to observe the predicted sharp lines in the $^{12}\text{C}(\pi^-, \gamma)^{12}\text{B}$ reaction (Fig. 1).

In the four years since then, the field has developed rapidly. Experimentally, the data have been extended to nuclei of the entire periodic table and several transitions to individual nuclear states isolated. The pionic x-ray data, needed to determine the capture orbitals and total strong absorption widths, have improved. Theoretically, the relative importance of various terms in the effective interaction has been further clarified and more realistic nuclear wave functions are being employed. These efforts, as will be seen, have shown radiative π capture to be a quantitative probe of nuclear structure.

Fig. 1. Photon energy spectrum from π^- capture in ^{12}C . (a) Spectrum with fitted function, using three Breit-Wigner forms plus the pole model for the continuum. (b) Photon spectrum for pions with a mean energy of 40 MeV used for in-flight background subtraction. (c) Spectrum with the pole model subtracted. The solid curve is the best fit; the dashed curve is the prediction of Kelly and Ueberall²⁷ for excitation of giant dipole states.

XBL 733-507

In addition to nuclear structure investigations, the experimental π^- capture matrix elements contribute to developing the theory which in the literature is termed the elementary particle treatment⁵ of nuclei. Here one tries to link together various weak and electromagnetic processes such as radiative and charge-exchange π capture, μ capture, β decay, γ decay, and electron scattering. The nuclear physics is contained in various invariant form factors of the vector and axial-vector weak hadronic currents. By making use of the conserved vector current (CVC) and partially conserved axial vector-current (PCAC) hypotheses, together with the soft pion limit ($q \rightarrow 0$), one can derive relationships between these rates. For example, it has been shown that radiative π capture from the $1s$ orbital is governed by the axial-vector form factor, which also appears (at a lower momentum transfer) in allowed Gamow-Teller β -transitions and in μ capture. This type of study was initiated in 1965 by Kim and Primakoff⁶ and has been advocated recently by numerous authors.⁵ At present only two transitions, in ^3He and ^6Li , have been carefully studied in this manner and these will be discussed. Two facts limit the greater application of this approach. In light nuclei, $2p$ -state capture dominates and for this orbit the soft-pion results do not obtain. Also, the need to have as input good experimental rates on the two states (or analogs) connected by π capture has restricted the application of this approach to a few cases.

EXPERIMENT

The process of radiative pion capture and the method of observation to be discussed occur in the laboratory in the following manner. A beam of 100-MeV pions, produced by bombarding a Be ribbon with 720-MeV protons, is brought to a focus at a point 10 m from production. The transit time is 4.1×10^{-8} sec, the pion lifetime is $\gamma \tau_{1/2} = 4.5 \times 10^{-8}$ sec. Before entering the target, the pions are degraded in energy by a ~ 25 -cm length of CH_2 and brought to rest in a target of

$1 - 4 \text{ g/cm}^2$. The slow-down time is $\sim 2 \times 10^{-9}$ sec. When the pion kinetic energy has dropped into the eV region it makes a transition to a negative energy atomic orbit of the nucleus to be studied. There it quickly (10^{-13} to 10^{-11} sec) makes 50 to 100 Auger or x-ray transitions until it reaches either the $1s$ state or a higher orbit which has sufficient overlap with the nucleus to make absorption competitive with x-ray transition. About 2% of the pions absorbed produce photons with energies centered around 120 MeV ($m_\pi = 139.6 \text{ MeV}$). The energy spectrum by measured by permitting the photons to impinge on a thin gold foil, part of a pair spectrometer, where 2.3% produce electron-positron pairs. The circular trajectories of this pair in an ~ 8 -kG field are measured at several points with wire spark chambers. The momenta thus measured are added to give the photon energy. The pair spectrometer⁴ employed in the measurements at the 184-inch Berkeley cyclotron gives a resolution (FWHM) of 2 MeV at 130 MeV. The overall efficiency (conversion $\times \Delta\Omega/4\pi$) is 4.15×10^{-5} at 130 MeV.

GENERAL ASPECTS OF THE PROBLEM

For orientation, let us look at some aspects of the physics involved which pertain to all nuclei and which are already evident from the ^{12}C study.

TREATMENT OF THE CONTINUUM

All spectra for nuclei with $A > 4$ and $A = 3$ exhibit a broad continuum with a maximum between 110 and 120 MeV. Compared to three-body phase space ($A_\pi\gamma$) the data are more sharply peaked (Fig. 5a); compared to a Fermi-gas model calculation^{1,4} the data are broader. A reasonably good description is given by the pole model of Dakhno and Prokoshkin⁷ which identifies the continuum with quasi-free capture on a proton. The single-pole diagram (discussed by Shapiro⁷ in the context of dispersion theory for direct nuclear interactions) and the expression for the photon spectrum are:

$$\text{amplitude} = \frac{G}{(t-m^2)},$$

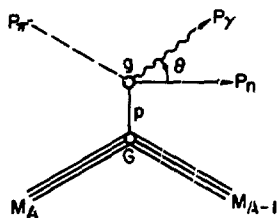
$$4\text{-momentum transfer: } t = (P_Y + P_n - P_\pi)^2,$$

$$\text{proton (neutron) [pion] mass} = m (m_n) [\mu]$$

proton separation parameter:

$$\Delta = M + m_n + E_{A-1}^* - M_{A'}.$$

E' 's = total energy.



KSL 734-2600

Fig. 2. Pole graph for radiative π^- capture.

$$\frac{dN(E_Y)}{dE_Y} = \text{const.} \times (G \cdot g)^2 \times E_Y^2 \int_{-1}^{+1} d(\cos \theta) \frac{E_n P_n^3}{(t-m^2)^2} \times \frac{E_{A-1}}{P_n^2 (M_{A-1} + \mu - E_Y) + P_n E_Y E_n \cos \theta}. \quad (3)$$

The curves shown with the data were computed with the above expression, which we evaluate numerically to include the complete kinematics. Since the normalization and the average excitation energy E_{A-1}^* of the recoil nucleus have not been given by theory, we choose values which give the best description of the data. The values of E_{A-1}^* determined in this manner are found to vary between 0 and 5 MeV. The pole model is clearly a first approximation: it ignores the motion of the proton in the nucleus and the final state interaction between the outgoing neutron and recoil nucleus. These are known to modify considerably the photon spectrum of ^2H and ^4He as discussed below. Nevertheless, one obtains a good description of the photon spectrum in many cases with particularly good results for ^3He and ^{14}N . Ultimately one hopes for a unified model which treats both quasi-free capture and the resonances on an equal footing.

THE EFFECTIVE HAMILTONIAN

The transition operator for radiative π capture is taken to be the nonrelativistic reduction of the photopion production amplitude on the nucleon (Chew et al. ⁴⁰). In applying this to nuclei in the impulse approximation (IA), and taking the pion to be bound in an atomic orbit $\phi_l^n(\vec{r})$, Delorme and Ericson² write this as

$$H_{\text{eff}} = \left(1 + \frac{m_\pi}{m_p}\right) \sum_{j,\lambda} e^{-\vec{k} \cdot \vec{r}_j} H_\lambda(j) \phi_l^n(\vec{r}), \quad (4)$$

where

$$\begin{aligned} H(j) = & 2\pi i t^+(j) [A \vec{\sigma}_j \cdot \hat{\epsilon}_\lambda + B (\vec{\sigma}_j \cdot \hat{\epsilon}_\lambda) (\vec{q} \cdot \vec{k}) \\ & + C (\vec{\sigma}_j \cdot \vec{k}) (\vec{q} \cdot \hat{\epsilon}_\lambda) + i D \vec{q} \cdot (\vec{k} \times \hat{\epsilon}_\lambda) \\ & + E (\vec{\sigma}_j \cdot \vec{q}) (\vec{q} \cdot \hat{\epsilon}_\lambda) \} \sigma(\vec{r} - \vec{r}_j). \end{aligned} \quad (5)$$

The transition rate (in units of $\hbar=c=1$) between initial (J_i) and final (J_f) nuclear states is given by

$$\begin{aligned} \Lambda_Y(nl; i \rightarrow f) = & \frac{k}{\pi} \frac{1}{(2J_i+1)(2l+1)} \\ & \times \sum_{m_i, m_f} \int \frac{d\vec{r}}{4\pi} | \langle J_f M_f | H_{\text{eff}} | J_i M_i \rangle |^2. \end{aligned} \quad (6)$$

In the above, $\vec{\sigma}_j$ and \vec{r}_j are the Pauli spin and coordinate of the j th nucleon and $t^+(j)$ is the isospin raising operator; i. e., $t^+ | \text{proton} \rangle = | \text{neutron} \rangle$. The photon polarization and propagation vectors are denoted by $\hat{\epsilon}_\lambda (\lambda = \pm 1)$, and \vec{k} and the pion momentum and coordinates are denoted by \vec{q} and \vec{r} . The effective coupling con-

[†]In practice one takes $\vec{q} \phi_l^n = -i \vec{\nabla} \phi_l^n$. The Fermi motion of the proton on which capture takes place is ignored. A discussion of this point can be found in Ref. 9.

stants A, B, C, D, and E are linear combinations of the electric and magnetic multipoles contributing to the $\gamma+n \rightarrow \pi^+p$ cross section at low energies. Threshold values have been given by numerous authors and some are listed in Table II. Although the most recent solutions (1972-73) are all based on the tables of Berends *et al.*¹² (1967), there are still some discrepancies in B, C, D, and E. Kawaguchi *et al.*⁸ determined their values by employing the CGLN⁴⁰ solution of the fixed- t dispersion relations and used as input pion-nucleon phase shifts. The fact that these values agree quite closely with the ones based on the work of Berends *et al.*, which reproduce photo production data, gives a rather consistent picture. The need for a sign change in the D term has just recently been suggested by Maguire and Wernitz⁹ and is corroborated by Nixon.¹⁰ Also, the kinematic factor $1 + m_\pi/m_p$ which appears in Eq. (4) but not in the work of Delorme and Ericson and Kawaguchi *et al.* is discussed in Ref. 9.

Most of the calculations for π -capture transitions have employed only the $A(\vec{\sigma} \cdot \hat{e}_\lambda)e^{i\vec{k} \cdot \vec{r}}$ terms of the Hamiltonian, since an estimate by Delorme and Ericson² indicated that the momentum-dependent terms play only a minor role for 1s, 2p, and 3d capture. This result was derived for the total (all final nuclear states) radiative capture rate by employing the Fermi gas model and closure over final nuclear states. Recent studies^{13, 14, 5} in which transitions to individual nuclear states were considered have shown that this conclusion is correct to within a few percent for 1s-state

capture; however, for 2p-state capture the momentum-dependent terms (B, C, D) make sizeable contributions. For example, in the $\pi^- + {}^6\text{Li} \rightarrow \gamma + {}^6\text{He}$ (g. s.) transition Vergados and Baer¹⁴ obtain a value $f = 0.7$ for the ratio of contributions to $\lambda_\gamma(2p)$ involving B and C terms to the A term only. The E term, quadratic in pion momentum, is expected¹⁴ to make negligible contributions to 1s and 2p capture, but may be important for 3d ($l \geq 2$) capture.

ROLE OF PIONIC X-RAY DATA

The physics of mesic atoms and the pionic x-ray data play an absolutely crucial role in the quantitative evaluation of theoretical π -capture matrix elements. Two quantities are needed: (1) probabilities, $\omega(nl)$, that the pion gets absorbed into the nucleus from the orbit (nl) and (2) total strong absorption rates $\Lambda_p(nl)$ of each orbit. The $\omega(nl)$ are related to the level population probabilities $P(nl)$ by

$$\omega(nl) = P(nl) \frac{\Lambda_a(nl)}{\Lambda_a(nl) + \Lambda_x(nl) + \Lambda_A(nl)}, \quad (7)$$

where $\Lambda_x(nl)$ [$\Lambda_A(nl)$] are the x-ray (Auger) transition rates for depopulating level nl . The $P(nl)$ are determined by atomic cascade calculations which fit to the x-ray intensity data. The $\Lambda_a(nl)$ are either measured directly from the broadening of x-ray lines or deduced indirectly from the x-ray intensity balance on level (nl) and the electromagnetic width. The fraction of pions undergoing radiative π -capture transitions at each

Table II. Coupling constants of the effective impulse approximation Hamiltonian (text) for radiative π^- capture transitions in nuclei.

	A ($10^{-3} m_\pi^{-2}$)	B ($10^{-3} m_\pi^{-4}$)	C ($10^{-3} m_\pi^{-4}$)	D ($10^{-3} m_\pi^{-4}$)	E ($10^{-3} m_\pi^{-4}$)
Delorme & Ericson ^a (1966)	-34±3	19	-17	-10	
Kawaguchi <i>et al.</i> ^b (1968)	-32	7.5	-37	-14	
Maguire & Wernitz ^c (1972)	-33.2	4.8	-32.9	+11.7	30.4
Nixon ^d (1973)	-33	5.5	-37	+13	30
Roig and Pascual ^f (1973)	-31.9	4.2	-29.5	-10.9	20.7
Schwela (1973) ^e	-31.7±.9	6.5±.2	-33.0±.9	+8.9±.6	

^a Ref. 2. ^b Ref. 8. ^c Ref. 9. ^d Ref. 10. ^e Ref. 10. ^f Ref. 11; values have been divided by $[1 + (m_\pi/m_p)]$ since H_{eff} of Ref. 11 differs by this factor from Eq. (4) in text.

orbital is $\omega(nl) \cdot \Lambda_Y(nl)/\Lambda_a(nl)$. Since nl is not fixed in the existing measurements of the radiative branching ratios (R_Y) one must perform the incoherent sum over all orbitals

$$R_Y = \sum_{nl} \frac{\Lambda_Y(nl)}{\Lambda_a(nl)} \omega(nl). \quad (8)$$

It is generally assumed that the ratio $\Lambda_Y(nl)/\Lambda_a(nl)$ depends only on l , not n . For light nuclei, capture occurs only from $l = 0$ and $l = 1$ orbits; therefore, the quantity

$$R_Y = \frac{\Lambda_Y(1s)}{\Lambda_a(1s)} \sum_n \omega(ns) + \frac{\Lambda_Y(2p)}{\Lambda_a(2p)} \times \sum_n \omega(np) \quad [\text{light nuclei}] \quad (9)$$

is compared with experiment. The role of p-state capture in light nuclei is often underestimated. The most recent studies indicate p/s state capture ratio $\left[\frac{\sum_n \omega(np)}{\sum_n \omega(ns)} \right]$ or 1.2 ± 0.3 (Ref. 15), 1.5 ± 0.4 , (Ref. 16) and 11.5 ± 4.5 (Ref. 16) for ${}^4\text{He}$, ${}^6\text{Li}$, and ${}^{12}\text{C}$, respectively. For ${}^1\text{H}$ and ${}^2\text{H}$ it is thought¹⁷ to be nearly zero.

RESULTS FOR NUCLEI WITH $1 \leq A \leq 4$

The photon spectra of all light nuclei studied thus far are displayed in Fig. 3 and results are summarized in Table III. [The only other possibility—an unstable target—is tritium, which the Berkeley group is planning to measure later this year at Los Alamos (LAMPF).] Since the emphasis here is primarily nuclear structure, we comment only briefly on each spectrum.

${}^1\text{H}$. The spectrum of hydrogen has played a central role in determining the basic properties of the pion and s-wave pion-nucleon interactions. In the present work it serves to calibrate the energy scale, instrumental line shape, and relative and absolute detection efficiency. The Panofsky ratio deduced for the spectrum shown in Fig. 3 a is 1.56 ± 0.10 , which agrees well with the currently accepted value of 1.53 ± 0.02 .

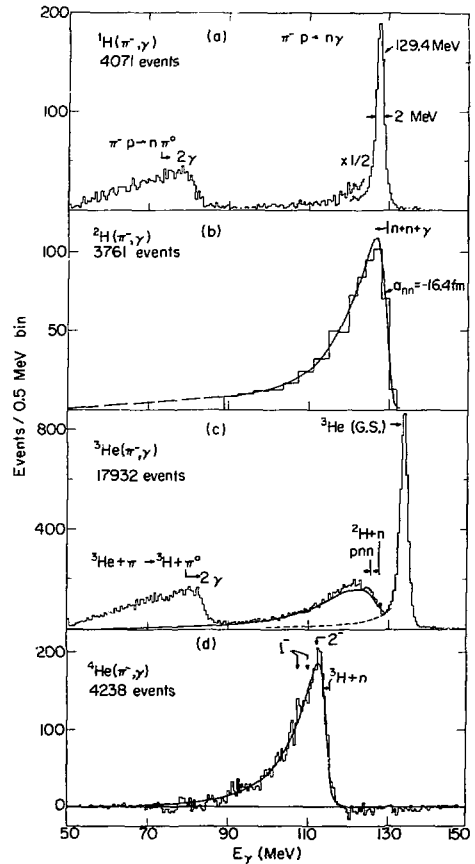


Fig. 3. Photon spectra for nuclei with $1 \leq A \leq 4$. (a) Spectrum for hydrogen (employed in the calibration of the pair spectrometer). (b) Spectrum for deuterium from Ryan.¹⁹ The curve is calculated for a 2-neutron ${}^1\text{S}$ -state scattering length $a_{nn} = -16.4$ fm. (c) Spectrum for ${}^3\text{He}$. The solid curve is a pole-model calculation. (d) Spectrum for ${}^4\text{He}$ by Bistirlich et al.⁴ The solid curve is an R-matrix calculation, assuming excitation of three states as indicated.

${}^2\text{H}$. The spectrum for deuterium was the first to demonstrate the usefulness of radiative π capture to nuclear physics. The spectrum (Fig. 3 b) is sharply peaked toward the high-energy end due to the

Table III. Summary of experimental values^a and some resulting interpretations for radiative absorption of stopped π^- on nuclei with $1 \leq A \leq 4$.

	¹ H	² H	³ He	⁴ He
Panofsky ratio P^g	$1.53 \pm .02$	$(3 \pm 4) \times 10^{-3}$	$2.28 \pm .18^b$	2.89 ± 0.15^d charge exchange Q-forbidden
Radiative branching (%) R_γ	$39.5 \pm .3$	$24.7 \pm .7$	$t\gamma : 6.9 \pm .5^b$ $dny : 3.6 \pm 1.2^c$ $pnny : \text{---}$ $tot : \text{---}$	6.5 ± 0.8^d $[7.4 \pm 1.7]^d$ 13.9 ± 1.9^d $1.50 \pm .09$
Nucleon emission (%) only	R_n^h Forbidden	$75.3 \pm .7$	73.7 ± 5.9^c	67.0 ± 2.6^d $98.5 \pm .09$ ${}^3H+n: 19.4 \pm 1.8^e$ 18.4 ± 1.4^f
	Identification and mass of π^0	Odd intrinsic parity of π	Structure of $A=3$ system and 3-body forces	T=1 structure of $A=4$ system; states with $J\pi = 2^-, 1^-, 1^-$ observed
Results	Link πN scattering to photoproduction at threshold πN coupling strength	Determine neutron s-wave scatt. length a_{nn} basic link in s-wave pion physics and πn production in N-N collisions	Test of PCAC and soft-pion theorem; relate π^- capture to β decay, μ capture and (ee') via axial-vector form factor	

^a Unless otherwise stated, references given in Table I. ^b Zaimidoroga *et al.*²² (1967). ^d Berkeley group. ^e Block *et al.*³⁸ (1963). ^f Zaimidoroga *et al.* quoted in Ref. 39.

$$g_p = \frac{\omega(\pi^- + A_i \rightarrow \pi^0 + A_f)}{\omega(\pi^- + A_i \rightarrow \gamma + A_f)} \quad h R_n = 1 - R_\gamma - P \cdot R_\gamma \text{ (g.s.)}$$

final-state n-n interaction. The shape of the spectrum near its maximum can be used to determine the n-n ¹S-wave scattering length a_{nn} . Watson and Stuart¹⁸ showed that for ¹s state capture of the pion energy dependence of the photon spectrum near the endpoint is given by

$$M^2 \propto \left| \frac{\sin \delta(p)}{p} \right|^2 \approx \frac{1}{(p^2 a^2 + 1)}; \quad (10)$$

$$p \cot \delta = -\frac{1}{a} + \frac{1}{2} r_0 p^2 + O(r_0^3 p^4)$$

where p is the relative neutron momentum, $a \equiv a_{nn}$ and r_0 is the effective range, assumed to be known from pp scattering. The curve shown in Fig. 2b was computed¹⁹ with $a_{nn} = 16.4$ fm and $r_0 = 2.65$ fm. The uncertainty in the ex-

tracted a_{nn} is approximately 3 fm. The currently accepted²⁰ value is $a_{nn} = -16.5 \pm 1.0$ fm.

³He. The spectrum for ³He, displayed in Fig. 3c, shows the presence of all four γ -ray channels discussed in the theoretical study of Messiah:²¹ (1) the $t + \gamma$ line at 135.8 MeV, (2) $d + \gamma$ continuum with an end-point energy of end-point energy of 129.8 MeV, (3) $p + n + n + \gamma$ continuum with an end-point of 127.7 MeV, (4) the $t + \pi^0$; $\pi^0 \rightarrow 2\gamma$ resulting in a uniform distribution of γ rays between 53 and 86 MeV. The relative strengths predicted by Messiah were 6.5/2.9/0.7/12.5 in the order listed above and normalized to our measured value of the $t\gamma$ channel (Table III). Our measurements do not resolve the $d\gamma$ and $pnny$ components, but if one uses the branching ratio for dny determined by Zaimidoroga *et al.*,²²

the respective ratios are $6.5 \pm 0.8 / 3.6 \pm 1.2 / 3.8 \pm 2 / 18.6 \pm 2.3$. This good agreement is remarkable considering that the calculation was performed more than 20 years ago.

The PCAC hypothesis and soft-pion theorem approach has been applied by Ericson and Figureau²³ to compute the radiative and charge exchange rates of the ${}^3\text{He}{}^3\text{H}$ system. They obtain 2.70 for the Panofsky ratio for 1s capture which agrees well with our measurement 2.89 ± 0.15 . Regarding p-state capture, for which there are no x-ray data, they estimate that 16% of the pions reaching the 2p orbit are absorbed. Of these only 0.1% and 0.03% undergo charge exchange and radiative transitions, respectively, to the triton. Thus the Panofsky ratio should not be affected. For the absolute radiative rate from the 1s orbit, they obtain $\lambda_\gamma(1s) = 3.46 \times 10^{15}$ sec. One would like to compare this with the measured ground state branching ratio but the needed p/s capture ratio has not been measured.

The region of the photon spectrum where the breakup channels (dny, pnny) dominate is shown in Fig. 4. The solid curve is a pole-model calculation with $\Delta = 6.8$ MeV corresponding to the dny vertex. It is normalized to the data in the 90- to 115-MeV region. This model, which neglects final-state interactions and the initial proton motion in ${}^3\text{He}$, is seen to give a good overall description. There is a suggestion of a broad peak in the region corresponding to 10- to 15-MeV excitation. This is the region where Chang et al.²⁴ suggest there exists a $T = 1/2$ state on the basis of their ${}^2\text{H}(p, \gamma){}^3\text{He}$ excitation function. The statistical evidence of our spectrum, which contains a factor of nearly 4 more counts than in the first published spectrum,²⁵ still falls short of being totally convincing. Clearly, a careful analysis with good theoretical calculations for the two breakup channels is needed before any conclusions can be reached.

⁴He. The radiative capture rate drops by one order of magnitude in going from ${}^3\text{He}$ to ${}^4\text{He}$; indeed, the value $1.50 \pm 0.09\%$ for ${}^4\text{He}$ is the lowest in Table I. The shape of the spectrum (Fig. 3d) is poorly described by the pole model, but can be entirely accounted for by assuming the excitation of three broad $T = 1$ resonances: 2^- at 3.4 MeV above the ${}^3\text{He}+n$ threshold;

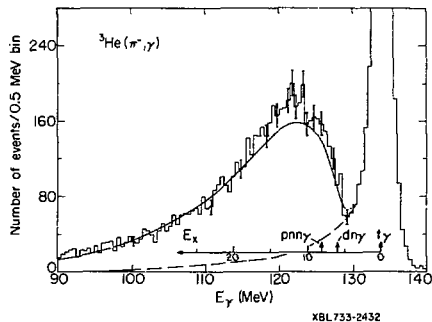


Fig. 4. Photon spectrum for ${}^3\text{He}$ in region where the breakup channels pnny and dny dominate. The solid line is a pole-model calculation as discussed in the text.

1^- at 5.1 MeV; 1^- at 7.4 MeV. The solid curve in Fig. 3d is based on an R-matrix calculation⁴ with the simple nuclear wave functions: $|2^-\rangle = |{}^3P_2\rangle$; $|1^-, \alpha\rangle = -0.782 |{}^1P_1\rangle + 0.625 |{}^3P_1\rangle$; $|1^-, \beta\rangle = -0.625 |{}^1P_1\rangle + 0.782 |{}^3P_1\rangle$. The mixing between the two 1^- states is not uniquely determined by the spectrum analysis. The total radiative transition rate⁴ based on the above wave functions, $\Lambda_\gamma(1s) = 7.18 \times 10^{14}$ sec⁻¹, compares well with the experimental value of 8.25×10^{14} sec⁻¹ which was obtained⁴ by assuming that p-state capture can be neglected. A more recent calculation by Raiche and Werntz¹⁵ which includes the p state, but neglects momentum-dependent terms in the transition operator, yields for the radiative branching ratio $R_\gamma = [(1.9)_s + (0.2)_p]\% = 2.1 \pm 0.7\%$. An interesting result of the later study was to demonstrate that the neutron- γ correlation depends strongly on the l of the pionic Bohr orbit. In the future this may provide an independent check on the capture probabilities $\omega(nl)$ determined from x-ray data.

RESULTS FOR 1p SHELL NUCLEI

The sensitivity of radiative π capture to the structure of individual nuclear states is most clearly seen in the photon spectra of 1p-shell nuclei, $4 < A \leq 16$. Examination of such spectra (Fig. 5) shows that the nuclear transition matrix elements are particularly large to certain bound and unbound states. We discuss these states separately, since the question of background subtraction and the accuracy of theoretical predictions are different.

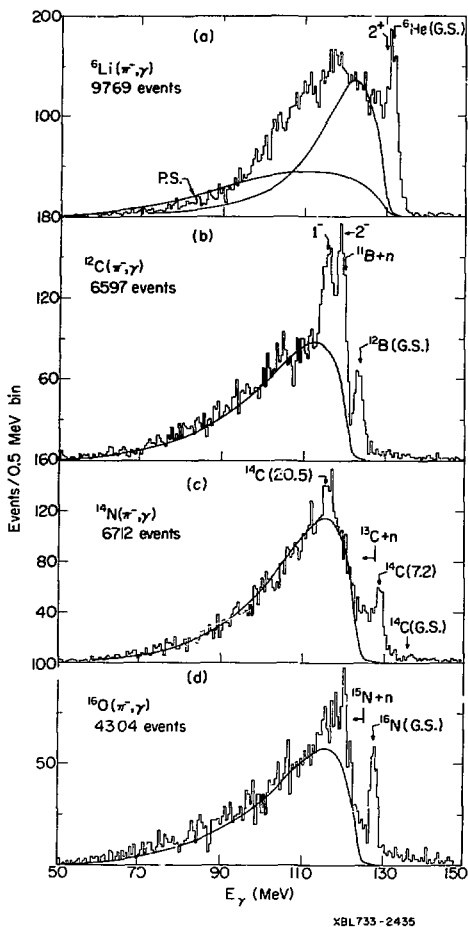


Fig. 5. Photon spectra for 1p-shell nuclei. Solid curves are pole-model calculations. The phase space curve (P. S.) in (a) is seen not to describe the continuum well.

GIANT RESONANCES

As was mentioned previously, the motivation for performing high-resolution radiative π -capture studies was based largely on interest in observing giant resonances, particularly the giant dipole (GD) states. The states to be observed are the $T_z = +1$ members of $T = 1$ isobaric triads whose $T_z = 0$ members are the giant resonances well known from

photonuclear and inelastic electron-scattering studies. Strong excitation of such states in π capture was predicted by Delorme and Ericson² (1966), Anderson and Eisenberg² (1966), and Überall² (1966). Bistirlich *et al.*⁴ first observed these states in the $^{12}\text{C}(\pi^-, \gamma)^{12}\text{B}$ reaction and their results are shown in Fig. 1. The spectrum shows three peaks at photon energies of 124.7, 120.3, and 116.9 MeV which were identified with transitions to 1^+ , 2^- , and 1^- states, respectively, in ^{12}B . The analogs in ^{12}C are at 15.1, 19.9, and 23.7 MeV. The solid curve in Fig. 1c shows the fit to the data assuming three Breit-Wigner forms. The data in this figure are what remain after subtraction of a contribution due to in-flight capture (transitions before π^- comes to rest) and the quasi-free component as given by the pole model.⁷ The dashed curve shows the spectrum predicted by Kelly and Überall,²⁷ using the ^{12}C wave functions of Kamimura *et al.*²⁷ These wave functions, tailored to describe the splitting of the GD state observed in the $^{11}\text{B}(p, \gamma)^{12}\text{C}$ reaction, couple the 2^+ state at 4.43 MeV in ^{12}C with the GD oscillation. When used to compute the π capture rates, they are seen to result in a qualitative description of the data.

Skupsky¹³ has improved the theoretical analysis of the ^{12}C data. He included the momentum-dependent terms in the transition operator of Eq. (5) and used nuclear wave functions for the giant resonances which coupled an s-d shell nucleon to low-energy states of the Cohen-Kurath model for ^{11}C . His calculations show that three states dominate photoexcitation, μ capture, and π capture: two 1^- levels computed to be at 22.4 and 25.9 MeV in ^{12}C , and one 2^- level at 20.6 MeV. The two 1^- states are largely responsible for the observed splitting of the GD strength in photoabsorption. The 2^- state, not seen in photoabsorption, dominates μ capture where its strength results entirely from the axial vector interaction. In π capture, all three levels are strongly populated and are identified with the peaks in the photon spectrum at 120.3 and 116.9 MeV. The predicted radiative branching ratios (Table IV) to these states are $R_\gamma(1^-) = 0.19\%$ and $R_\gamma(2^-) = 0.28\%$. The value of Bistirlich *et al.*⁴ are $R_\gamma(1^-) = 0.159 \pm 0.016\%$ and $R_\gamma(2^-) = 0.185 \pm 0.019\%$. A likely explanation for the discrepancy in $R_\gamma(2^-)$ is that in the experimental determination the pole-model subtraction is too large. If no pole-model subtraction is

Table IV. Comparison of experimental and theoretical radiative π -capture branching ratios in 1p-shell nuclei.

Nuclei $ T_z=0\rangle \rightarrow T_z=1\rangle$	J_i^π	J_f^π	Experiment ^a			Shell model		Other models
			$E_x(T_z=1)$ (MeV)	$E_x(T_z=0)$ (MeV)	R_γ (%)	R_γ (%)	Valence Orbitals	R_γ (%)
${}^6\text{Li} \rightarrow {}^6\text{He}$	1^+	0^+	0.0	3.56	.306±.035	.36 ^b	1p	.41±.11 ^c
		2^+	1.8	5.36	.148±.025	.08 ^b	1p	
${}^{12}\text{C} \rightarrow {}^{12}\text{B}$	0^+	$(1^+, 2^+, 2^-)$.35	15.45	.091±.009	.07 ^d	1p, 2s, 1d	.105±.035 ^c
		2^-	4.75	19.85	.185±.019(.30) ^e	.28 ^c	1p, 2s, 1d	
		1^-	8.10	23.20	.159±.016(.42) ^e	.19 ^f	1p, 2s, 1d	
${}^{14}\text{N} \rightarrow {}^{14}\text{C}$	1^+	0^+	0.0	2.31	<.008	.008 ^h	1p	
		2^+	7.01	9.17	.094±.024	.12 ^h	1p	
		2^-	7.34	9.51		.009 ^h	1p, 2s, 1d	
		Giant res.	20.5	22.8				
${}^{16}\text{O} \rightarrow {}^{16}\text{N}$	0^+	$(2^-, 0^-, 3^-, 1^-)$	0.0	13.0	.15±.03	.168 ^k	{ 1p, 2s, 1d 2p, 1f	
		2^-	7.70	20.7	.22±.05(.58) ^g			.43 ⁱ
		GD + GQ	5.6-15.6	18.6-28.6	.25±.06(.97) ^g		1.65 ^j	

^a Berkeley group.³ ^b Vergados and Baer¹⁴ (1972). ^c Maguire and Werntz⁹ (1972). ^d Skupsky¹³; includes only 2^- state at $E_x = 5.1$ MeV.

^e Skupsky¹³; 1^- states at $E_x = 7.0, 7.5, 10.5$ MeV, ^g Assume pole-model contribution = 0. ^h Vergados³¹ (1972).

ⁱ Murphy *et al.*²⁸ (1967); transition to 2^- state predicted at 17.5 MeV in ${}^{16}\text{O}$.

^j Murphy *et al.*²⁸ (1967); sum of contributions to GD states ($0^-, 1^-, 2^-$) and GQ states ($1^+, 2^+, 3^+$) between 17.5 and 29.1 MeV in ${}^{16}\text{O}$.

^k Werntz³⁰ (1971).

made, one obtains 0.30%—much closer to the theoretical value.

In ^{16}O , the giant quadrupole resonances ($L=2$, $S=1$, $T=1$) were predicted to be important by Murphy *et al.*²⁸ Using a generalized Goldhaber-Teller model, they showed that for $1s$ capture the photon spectra of π capture are dominated by giant dipole states, for $2p$ capture by giant quadrupole (GQ) states (1^+ , 2^+ , 3^+). Since more than 90% of the pions are captured from p orbitals, it was hoped that evidence for these not-too-well-established collective modes could be found. Unfortunately, the spectrum in the region of the GQ states, $E_\gamma = 111.5$ to 121.5 MeV, shows no easily identified resonances. Bistirlich *et al.*⁴ get a branching ratio of $\sim 0.25\%$ for the strength to this region after they subtract the non-resonant component by the pole model. Murphy *et al.* get 1.65% for the total strength to $\overline{\text{GD}}$ and GQ states in this region. If one assumes in the determination of the experimental number that the quasi-free component is zero in this region, the branching ratio is 0.97% which is closer to the theoretical estimate. Nevertheless, one must say that the evidence is inconclusive. It would be useful to have a calculation for GQ states, using the full Hamiltonian and better nuclear wave functions.

The preliminary results of ^{14}N (Fig. 5c) show a resonance-like peak at 20.5 MeV in ^{14}C (22.8 MeV in ^{14}N). It will be interesting to see if the prediction by Murphy *et al.* that GQ excitations dominate when the pions get captured predominantly from $l = 1$ orbits can be verified. The subtraction of the quasi-free background may be clearer in ^{14}N since, unlike ^{12}C and ^{16}O , this component seems to extend on both sides of the resonance. One sees that a larger value of the excitation energy of the recoil nucleus $E_x = \Delta - \Delta$ (min) must be used in the pole model. For the curve shown in Fig. 5c, $E_x = 3.9$ MeV. In the ^{12}C and ^{16}O analysis, $E_x = 0$ and 1.6 MeV respectively were employed. The fit to the ^{14}N data given by the pole model is excellent (the full analysis of this spectrum is still in progress). The larger Δ needed in ^{14}N suggests that the ^{12}C and ^{16}O data may require a large Δ . As discussed above, this would improve the agreement with theory on giant-resonance excitation.

Giant-dipole states have not been

identified in the mass-6 system. The suggestion of a peak occurs at $E_\gamma = 119$ MeV (Fig. 5a). This is at 15.6 MeV relative to the ^6He ground state and 3.3 MeV above the threshold for breakup of ^6He into two tritons. Possibly, the observed structure is related to this channel. There are suggestions of other resonances in the spectrum, but the statistical evidence is weak. One can see that the pole model does not describe the data as well as for the other $1p$ shell nuclei. The spectrum expected for quasi-free capture on a deuteron in ^6Li has recently been calculated²⁹ (not shown). The photon spectrum for this capture mode makes relatively large contributions to the 90- to 120-MeV region, the region where the pole model for quasi-free capture on a proton deviates most from the data. A more complete study²⁹ of quasi-free capture on heavier clusters such as deuteron, and α -particles is in progress.

BOUND STATES

Since the nuclear structure of bound states is much better understood theoretically, and the experimental branching ratios are nearly free from uncertainties in background subtraction, one hopes for a precise evaluation of radiative π -capture theory. This is particularly true for the odd-odd nuclei ^6Li and ^{14}N where transitions to individual states can be resolved.

In the ^{12}C study, the ground state group (Fig. 1) is in the region of the 1^+ , 2^+ , and 2^- states in ^{12}B at 0.0, 0.95, and 1.67 MeV, respectively. The measured excitation energy, 0.35 ± 0.05 MeV, shows that the 1^+ transition dominates, but that there is a non-negligible contribution from one or both of the other two states. Skupsky¹³ obtains (Table IV) for the branching ratios $1^+ | 2^+ | 2^- |$ sum the values, in %, $0.045 | 0.021 | < 0.01 | 0.066$. Maguire and Werntz⁹ obtain $0.054 | 0.036 | 0.014 | 0.105$, respectively. The agreement with the measurement $R_\gamma(\text{sum}) = 0.091 \pm 0.009$ is seen to be quite good, but one would like better x-ray data on the $2p$ state before making final judgements.

For ^{16}O there have not been many theoretical calculations for the bound state transitions. The observed ground state group fully spans the region of the 2^- , 0^- , 3^- , and 1^- states in ^{16}N at 0.0, 0.12, 0.30, and 0.40 MeV, respectively. The measured branching for the sum of

states is $0.11 \pm 0.02\%$. A theoretical value of 0.168% was given by Werntz,³⁰ using the wave functions of Szydlik and Philpot.³⁰

The ^{14}N spectrum provides a unique possibility for studying π capture: the combination of high neutron separation energy ^{14}C (8.2 MeV) and high excitation energy of the first excited state in ^{12}C (1^- , 6.1 MeV) permits the ground state to be completely resolved. One sees in Fig. 5c that the transition is extremely weak. The β transition between the two states exhibits the well-known anomaly, i. e., $\log ft = 9$ rather than 3 as expected for an allowed Gamow-Teller transition. The radiative π -capture transition from the $1s$ -state also predominantly a Gamow-Teller transition (but at a higher momentum transfer), might therefore be expected to be small. The radiative p -state capture is apparently also small, judging from the small upper limit $R_{\gamma} < 8 \times 10^{-5}$ set by the experiment. Vergados³¹ analyzed this transition with shell-model wave functions and obtained $R_{\gamma}(0^+) = 7.7 \times 10^{-5}$. The other bound state peak seen in the spectrum is at 7.2 MeV excitation in ^{14}C . In this region there is 2^+ and 2^- state at 7.01 and 7.34 MeV, respectively. Vergados³¹ predicts (Table IV) that the 2^+ state completely dominates this region. The combined strength, 0.13%, compares well with the measured value $0.094 \pm 0.024\%$. In addition, Vergados finds that all other states below 9.5 MeV in ^{14}C make small contributions to the spectrum.

PCAC AND SOFT-PION APPROACH COMPARED WITH IA CALCULATIONS AND DATA IN ^6Li .

The transition $\pi^- + ^6\text{Li}(1^+) \rightarrow \gamma + ^6\text{He}(0^+, \text{g. s.})$ provides an important test of the PCAC hypothesis and soft-pion theorem approach (EP) for complex nuclei. The necessary input for the prediction of the $1s$ radiative capture rate $\lambda_{\gamma}(1s)$ is available: the β -decay and μ -capture rates are measured, the 0^+ analog state in ^6Li at 3.562 MeV has a well measured γ -decay width, and the electron scattering to this state has been measured by several groups. Thus a reasonably good determination of the axial vector form factor is possible. The experimental π -capture branching ratio has been determined by Deutsch et al.³² and the Berkeley group.³³

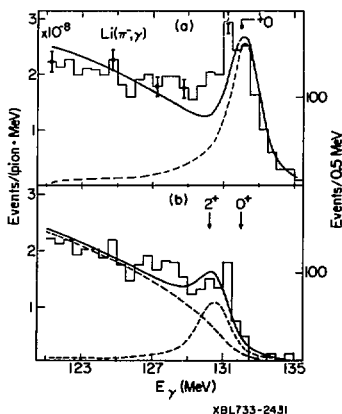


Fig. 6. High-energy end of ^6Li spectrum. (a) Single-line fit; dashed curve shows instrumental line shape. (b) Data after subtraction of ground state line; dashed curves: assumed shape of continuum and line at $E_x = 1.80$ MeV corresponding to excitation of 2^+ state.

The photon spectrum in the region of the 0^+ state is shown in Fig. 6. The comparison of the instrumental line shape with the peak in the ^6Li spectrum indicates that the latter is too broad for a single transition. A careful analysis³³ indicates that one must assume population of the 2^+ state at 1.8 MeV as shown in Fig. 6b. The uncertainty that the presence of the 2^+ state introduces on the extraction of the ground state is small, since we can normalize a single line to the ^6Li spectrum above 132 MeV where the contribution from other channels is small.

Four groups of authors have used the PCAC hypothesis and the soft-pion limit to compute $\lambda_{\gamma}(1s)$. These are given in Table V together with the results of Maguire and Werntz,⁹ who use the IA Hamiltonian but relate the nuclear matrix elements to other measured rates, and the shell model calculations of Roig and Pascual¹¹ and Vergados and Baer.¹⁴

We note these points:

(1) $\lambda_{\gamma}(1s)$: The EP values agree in general with IA values; however, the average EP value (excluding the 1968 estimate, which did not include some corrections) $\lambda_{\gamma}(1s) = 2.03 \times 10^{15} \text{sec}^{-1}$ is higher than the average IA value $1.46 \times 10^{15} \text{sec}^{-1}$. The EP value of Delorme³⁴ (2.3 ± 0.5) $\times 10^{15} \text{sec}^{-1}$ is the highest.

Table V. Radiative transition rates and branching ratios for $\pi_{\text{stop}}^- + {}^6\text{Li}(1^+) \rightarrow {}^6\text{He}(0^+) + \gamma$

Method	Transition rates		Branching ratios ^a			Reference
	$\lambda_\gamma(1s)$	$\lambda_\gamma(2p)$	R_s	R_p	$R_\gamma(s+p)$	
	10^{15} sec^{-1}	10^{10} sec^{-1}	(%)	(%)	(%)	
PCAC	1.65		.289±.118			Griffiths, Kim (1968) ³⁴
+	1.86 ± .18		.326±.134			Pascual, Fujii (1970) ³⁴
soft pions	1.9 + .4 - .2		.333±.136			Fulcher, Eisenberg (1970) ³⁴
	2.3 ± .5		.404±.166	.312±.047	.716±.171	Delorme (1970) ³⁴
IA	1.51 ± .15	5.26 ± .06	.265±.109	.138 ± .043	.403±.117	McGuire, Werntz (1972) ⁹
IA	1.46 ± .22	4.12 ± .62	.256±.105	.108 ± .033	.364±.111	Pascual, Roig (1972) ¹¹ ; $a = 1.98 \text{ fm}$
+	2.08	4.32	.365±.150	.113 ± .035	.478±.154	Vergados, Baer (1972) ¹⁴ ; $a = 1.66 \text{ fm}$
Shell model	1.40	4.44	.248±.101	.117 ± .036	.365±.107	Vergados, Baer (1972) ¹⁴ ; $a = 1.94 \text{ fm}$
Average (IA) ^b	1.46	4.61	.256±.105	.121±.037	.378±.111	
Experiment					1.0 ± .1 .306 ± .035	Deutsch <i>et al.</i> (1968) ³² Baer <i>et al.</i> (1973)

^a Indicated uncertainties in R are due to x-ray data only; use values $16 \sum_{\text{H}} \omega(ns) = .40(1\pm.23)$, $\sum_{\text{H}} \omega(np) = .60(1\pm.15)$.

$\Lambda_s(1s) = 2.28(1\pm.33) \times 10^{17} \text{ sec}^{-1}$ (Ref. 16), $\Lambda_p(2p) = 2.28(1\pm.27) \times 10^{15} \text{ sec}^{-1}$ (Ref. 16).

^b Average of impulse approximation (IA) calculations, excluding the value of Ref. 14 with $a = 1.66 \text{ fm}$ (1p-shell harmonic oscillator size parameter).

(2) $\lambda_{\gamma}(2p)$: Since the soft-pion limit does not apply to $2p$ capture, only IA values are available. All estimates in Table V except that of Delorme's are close to the average $\lambda_{\gamma}(2p) = 4.61 \times 10^{10} \text{ sec}^{-1}$ (excluding that of Ref. 34).

(3) R_{γ} : The average IA value $0.378 \pm 0.111\%$ agrees with our value $0.306 \pm 0.035\%$ but disagrees with the $1.0 \pm 0.1\%$ of Deutsch *et al.* 32

(4) Extracted $\lambda_{\gamma}(1s)$: By relying on the IA estimate for $\lambda(2p)$, one can extract $\lambda_{\gamma}(1s)$,

$$\lambda_{\gamma}(1s) = \frac{R_{\gamma}(\text{expt.}) - R_{\gamma}(\text{IA})}{\omega_s} \times \lambda_{\gamma}(1s)$$

$$= (1.05 \pm 0.52) \times 10^{15} \text{ sec}^{-1}.$$

This is in agreement with IA estimates but somewhat lower than the EP values.

In conclusion, we can say that at the present level of comparison between theory and experiment, no major discrepancies with either the EP or IA calculations are seen. Clearly more precise x-ray data are desirable. As these become available it should be possible to extract a precise value of $\lambda_{\gamma}(1s)$ which would test with greater accuracy the PCAC hypothesis and soft-pion approach.

MEDIUM-MASS AND HEAVY NUCLEI

All high-resolution data now available on nuclei with $A > 16$ are displayed in Fig. 7. The very preliminary data on ^{209}Bi is first presented here. The total radiative capture rates (Table I) are nearly the same for these three nuclei, although the capture orbitals are different. The Bohr radii ($r_B = 200 \text{ m}^2/2 \text{ fm}$) and nuclear radii ($r_N = 1.2 A^{1/3} \text{ fm}$) in order $^{24}\text{Mg}(2p)$, $^{40}\text{Ca}(3d)$, $^{209}\text{Bi}(5g)$ are 67, 90, 60 fm and 3.5, 4.1, 7.1 fm, respectively. One sees that the average distances between the pion and the proton when the interaction occurs do not vary greatly in these nuclei.

The photon spectra do not clearly show excitation of individual nuclear levels. However, one can see for ^{24}Mg and ^{40}Ca that there is considerable strength to the bound states. One cannot help feeling that if the spectra were recorded with a

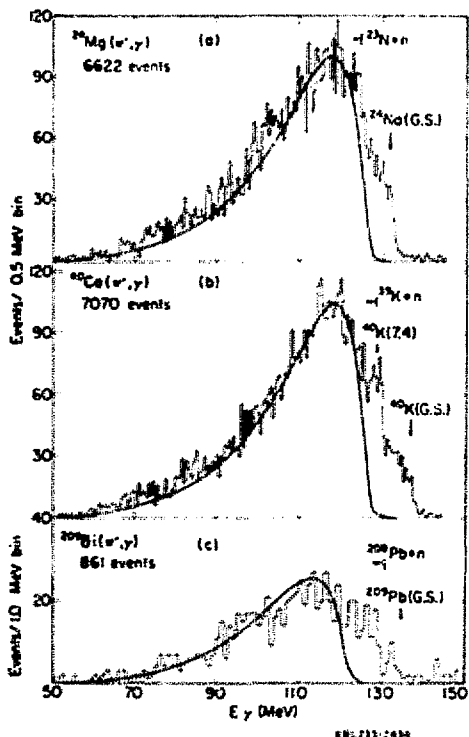


Fig. 7. Photon spectra for medium-mass and heavy nuclei. The curves are pole-model calculations. Evidence for excitation of the bound states of ^{24}Na and ^{40}K can be seen clearly.

resolution closer to that achieved in low-energy nuclear physics, say 300 keV, a new and rich spectroscopy of nuclear states would emerge. The fact that the basic transition operator is much better understood than, for example, the much used (p, p') reaction at 50 MeV, would make it a very powerful tool for nuclear structure investigations. With higher intensity pion beams soon to become available, the prospects seem favorable for obtaining 300-keV resolution with a pair spectrometer making use of a thinner converter foil.

The authors wish to thank Drs. John Vergados, Gary Nixon, and Carl Werntz for communicating unpublished results and for numerous helpful discussions.

REFERENCES

- ¹H. Davies, H. Muirhead, and T. N. Woods, Nucl. Phys. 78, 673 (1966).
- ²J. Delorme and T. E. O. Ericson, Phys. Letters 21, 98 (1966); D. S. Anderson and J. M. Eisenberg, Phys. Letters 22, 164 (1966); H. Überall, Nuovo Cimento Suppl. 4, 781 (1966).
- ³Berkeley group (past and present): J. A. Bistirlich, N. de Botton, S. C. Cooper, J. A. Helland, A. S. L. Parsons, Paul Skarek, P. Truđl and the authors.
- ⁴J. A. Bistirlich et al., Phys. Rev. Letters 25, 689 (1972); ibid. 25, 950 (1972); Phys. Rev. C 5, 1867 (1972).
- ⁵Reviewed by M. Ericson and M. Rho, Phys. Reports 5C, 59 (1972).
- ⁶C. W. Kim and H. Primakoff, Phys. Rev. 139, B1447 (1965).
- ⁷L. G. Dakhno and Yu. O. Prokoshkin, Sov. J. Nucl. Phys. 7, 351 (1968); I. S. Shapiro, Selected Topics in Nuclear Theory (IAEA, Vienna 1963), p. 85 ff.
- ⁸M. Kawaguchi et al., Prog. Theor. Phys. Suppl. (Kyoto), Extra No. 28.
- ⁹W. Maguire and C. Werntz, Nucl. Phys., in press.
- ¹⁰G. Nixon, private communication (1973); D. Schwela, private communication to P. Truđl (1973).
- ¹¹F. Roig and P. Pascual, preprint, G. I. F. T. (Spain) (April 1972).
- ¹²F. A. Berends, A. Donnachi, and D. Weaver, Nucl. Phys. B4, 1 (1967).
- ¹³S. Skupsky, Phys. Letters 36B, 271 (1971); Nucl. Phys. A178, 289 (1971).
- ¹⁴J. D. Vergados and H. W. Baer, Phys. Letters B41, 560 (1972); J. D. Vergados, private communication.
- ¹⁵A. Raiche and C. Werntz, Phys. Rev. C 4, 2003 (1971), and references therein.
- ¹⁶W. W. Sapp et al., Phys. Rev. C 5, 690 (1972); R. J. Harris et al., Phys. Rev. Letters 20, 505 (1969).
- ¹⁷M. Leon, Phys. Letters 37B, 87 (1971).
- ¹⁸K. M. Watson and R. N. Stuart, Phys. Rev. 82, 738 (1951).
- ¹⁹J. W. Ryan, Phys. Rev. 130, 1554 (1963).
- ²⁰H. Brückman, (rapporteur), Int. Conf. on Few Part. Prob. Nucl. Int., Los Angeles, 1972.
- ²¹A. M. L. Messiah, Phys. Rev. 87, 639 (1952).
- ²²O. A. Zaimidoroga et al., Soviet Phys. (JETP) 21, 848 (1965); ibid. 24, 1111 (1967).
- ²³M. Ericson and A. Figureau, Nucl. Phys. B3, 609 (1967).
- ²⁴C. C. Chang, E. M. Diener, and E. Ventura, Phys. Rev. Letters 29, 307 (1972).
- ²⁵H. W. Baer et al., Int. Conf. Few Part. Prob. Nucl. Int., Los Angeles, 1972.
- ²⁷F. J. Kelly and H. Überall, Nucl. Phys. A118, 302 (1968); M. Kamimura et al., ibid. A95, 129 (1967).
- ²⁸J. D. Murphy et al., Phys. Rev. Letters 19, 714 (1967).
- ²⁹G. Nixon et al., Bull. Am. Phys. Soc. 1973 (Washington)
- ³⁰C. Werntz, invited paper, Am. Phys. Soc. meeting, Tuscon, 1971; nuclear wave functions from P. Szydlik and I. Philpot, Phys. Rev. 153, 1039 (1967).
- ³¹J. D. Vergados, contribution to this conference.
- ³²J. Deutsch et al., Phys. Letters 26B, 315 (1968).
- ³³H. W. Baer et al., to be submitted to Phys. Rev.
- ³⁴J. Delorme, Nucl. Phys. B13, 573 (1970); L. P. Fulcher and J. M. Eisenberg, ibid. B18, 271 (1970); P. Pascual and A. Fujii, Nuovo Cimento 65A, 411 (1970); Erratum 67A, 135 (1970).
- ³⁵G. Backenstoss, Ann. Rev. Nucl. Science 20, 467 (1970).
- ³⁶W. Chinowsky and J. Steinberger, Phys. Rev. 100, 1476 (1955).
- ³⁷V. I. Petrukhin and Yu. D. Prokoshkin, Nucl. Phys. 54, 414 (1964).
- ³⁸M. M. Block et al., Phys. Rev. Letters 11, 301 (1963).
- ³⁹T. I. Kopaleishvili, Particles and Nuclei 2 (part 2), 87 (1973).
- ⁴⁰G. F. Chew et al., Phys. Rev. 106, 1345 (1957).